LODZ UNIVERSITY OF TECHNOLOGY

FACULTY OF MECHANICAL ENGINEERING

DEPARTMENT OF DYNAMICS

inż. Piotr Brzeski
170295

MASTER OF SCIENCE THESIS

Mechanical Engineering: Mechanical Engineering & Technology

Full-time studies

DYNAMICS OF THE PENDULUM SUSPENDED ON THE FORCED DUFFING OSCILLATOR

supervisor:
prof. dr hab. inż. Tomasz Kapitaniak

Contents

Chapter 1

Introduction

The dynamics of the pendulum or systems containing the pendulum is probably one of the oldest scientific topics. Simple parametrically excited pendulum shows extremely complex behaviour [1, 2]. Miles [3] shows that for the pendulum the route to chaos leads through symmetry breaking pitchfork bifurcation and cascades of period doubling bifurcations. Comprehensive analytical investigation of the pendulum with different forcing was presented by Bryant and Miles [4, 5, 6]. In the forced system one can consider two main parameters: the amplitude and the frequency of excitation. Such a bifurcation diagram for parametrically forced pendulum with horizontally moving point of the suspension was presented by Bishop and Clifford for periodic oscillations (PO) [7] and for periodic rotations (PR) [8]. In [9] bifurcation analysis was extended to elliptic movement of suspension point both for PO and PR. The analytical investigation of oscillating and rotating motions of pendulum was done using averaging, small parameter, harmonic balance, and other methods[10, 13, 14, 7, 15, 16, 17, 18, 19]. This analysis allows understanding of the pendulum dynamics in the neighbourhood of the locked periodic solutions. The interesting effect can be observed when the symmetry of the pendulum is broken, i.e., the imperfection term is added to the potential function [20]. In such an asymmetric system the symmetry breaking pitchfork bifurcation disappears and the sudden decrease of the amplitude of the PO at the first period doubling bifurcation can be regarded as a precursor of an escape or problems with system behaviour.

The crucial point in modelling of such systems is a good approximation of damping coefficients (viscous and frictional damping). There are well known methods for linear [11, 12] systems but as far as the pendulum is oscillating with large amplitude, the linear approximation does not give sufficient results. This problem has been solved by Xu et al. [21, 22]. They show an efficient method to extract the damping

coefficients (viscous damping and dry friction) from time series of freely oscillating pendulum and consider the influence of the shaker (the source of the forcing).

Most previous works on the dynamics of the pendulum suspended on the forced oscillator consider the linear oscillators. Such a system can be considered as a modification of the classical tuned mass absorber [23, 24]. Early works [25, 26] give approximate results by the method of harmonic balance in the primary parametric instability zone, which allows calculation of the separate regions of stable and unstable harmonic solutions. Further analysis allows to understand of the dynamics around primary and secondary resonances [27, 28, 29, 30, 31]. In the recent work Ikeda proposed the usage of two pendulums mounted in the same pivot as a tuned mass absorber [37]. His experimental results show good agreement with the numerical simulations and his model can be considered as a good alternative to one pendulum on the pivot in the design of tuned mass absorbers.

A good understanding of dynamics of tuned mass absorber with linear base system gives possibility to extend investigation to systems with non–linear base. Non–linearity in considered class of systems is usually introduced by changing the linear spring into non–linear one [32, 33] or magnetorheological damper [34]. In a few papers on this topic one can find an analytical study of the dynamics of Duffing – pendulum systems around principal and secondary resonances [30, 32, 33, 35, 36]. The main conclusion coming from the above mentioned papers is that non-linear spring in the base system causes enlargement of parameters range where pendulum can be used as a tune mass absorber.

In this thesis the pendulum suspended on the forced non–linear Duffing oscillator is considered. The purpose of analysis is to study the emergence and the stability of PO and PR in two parameters space: the amplitude and the frequency of excitation. Identification of the regions with one stable periodic solution, several coexisting periodic solutions, quasi-periodicity and chaotic behaviour is done.

The thesis is organized as follows. In Section 2 the dimensionless equations of motion are formulated. The possible scenarios of pendulum's destabilization are presented in Section 3. Section 4 shows two-dimensional bifurcation diagrams for PO, PR, as well as one-parameter continuations for representative values of parameters. The influence of non–linearity of spring on absorbing properties of the pendulum is studied as well. Section 5 shows the regions in two-dimensional parameter space where one, two, or several coexisted attractors can be observed. Finally, in Section 6 summarization of our results is done.

The thesis is realized within the TEAM programme of Foundation for Polish Science, co-financed from European Union, Regional Development Fund.

Chapter 2

Model of the system

The analyzed system is shown in Fig. 2.0.1. It consists of a Duffing oscillator with a suspended pendulum. The Duffing system is forced by periodical excitation and moving in a vertical direction. The position of mass M is given by coordinate y and the angular displacement of pendulum (position of the mass m) is given by angle φ. The equations of motion can be derived using Lagrange equations of the second type. The kinetic energy T, potential energy V, and Rayleigh dissipation D are given respectively by the following equations:

$$T = \frac{1}{2}(M+m)\dot{y}^2 - ml\dot{y}\dot{\varphi}\sin\varphi + \frac{1}{2}ml^2\dot{\varphi}^2, \tag{2.0.1}$$

$$V = \frac{1}{2}k_1y^2 + \frac{1}{4}k_2y^4 + mgl(1-\cos\varphi), \tag{2.0.2}$$

$$D = \frac{1}{2}c_1\dot{y}^2, \tag{2.0.3}$$

where M is mass of the Duffing oscillator, m is mass of the pendulum, l is length of the pendulum, k_1 and k_2 are linear and non–linear parts of spring stiffness, and c_1 is a viscous damping coefficient of the Duffing oscillator. The generalized forces are given by the following formula:

$$Q = F(t)\frac{\partial y}{\partial y} + Tq(\dot{\varphi})\frac{\partial \varphi}{\partial \varphi}, \tag{2.0.4}$$

where $F(t) = F_0\cos\nu t$ is a periodically varying excitation with amplitude F and frequency ν, $Tq(\dot{\varphi}) = c_2\dot{\varphi}$ is a damping torque with damping coefficient c_2. The damper of pendulum is located in a pivot of the pendulum (not shown in Fig. 2.0.1).

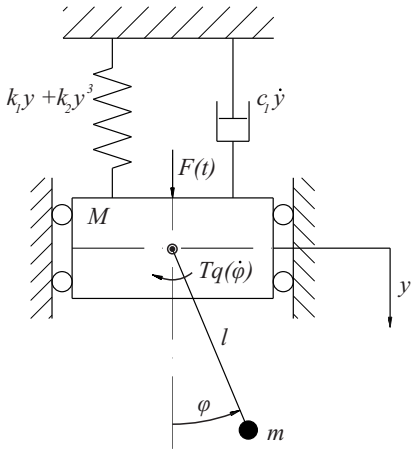

Figure 2.0.1: Model of system.

The damping in the pivot of pendulum is composed of viscous and dry friction damping [21]. Here dry friction component is neglected (to have a continuous system) and small value of viscous part is assumed(1% of critical damping). Such assumption does not change system dynamics.

One can derive two coupled second order differential equations:

$$(M+m)\ddot{y} - ml\ddot{\varphi}\sin\varphi - ml\dot{\varphi}^2\cos\varphi + k_1y + k_2y^3 + c_1\dot{y} = F_0\cos\nu t, \tag{2.0.5}$$

$$ml^2\ddot{\varphi} - ml\ddot{y}\sin\varphi + mlg\sin\varphi + c_2\dot{\varphi} = 0. \tag{2.0.6}$$

In the numerical calculations the following values of Duffing oscillator's parameters are used: $M = 5.0\,[\mathrm{kg}]$, $k_1 = 162.0\left[\frac{\mathrm{N}}{\mathrm{m}}\right]$, $k_2 = 502.0\left[\frac{\mathrm{N}}{\mathrm{m}}\right]$, $c_1 = 3.9\left[\frac{\mathrm{Ns}}{\mathrm{m}}\right]$ and the following values of the pendulum's parameters: $m = 0.5\,[\mathrm{kg}]$, $l = 0.1\,[\mathrm{m}]$, $c_2 = 0.001\,[\mathrm{Nms}]$. Static deflection of mass M is neglected.

Introducing dimensionless time $\tau = t\omega_1$, where $\omega_1^2 = \frac{k_1}{M+m}$ is natural linear frequency of Duffing oscillator, dimensionless equations of the form as follows can be reached:

$$\begin{gathered}\ddot{x} - ab\ddot{\gamma}\sin\gamma - ab\dot{\gamma}^2\cos\gamma + x + \alpha x^3 + d_1\dot{x} = f\cos\mu\tau,\\ \ddot{\gamma} - \tfrac{1}{b}\ddot{x}\sin\gamma + \sin\gamma + d_2\dot{\gamma} = 0,\end{gathered} \tag{2.0.7}$$

where $\omega_2^2 = \frac{g}{l}$, $a = \frac{m}{M+m}$, $b = \left(\frac{\omega_2}{\omega_1}\right)^2$, $\alpha = \frac{k_2 l^2}{(M+m)\omega_1^2}$, $f = \frac{F_0}{(M+m)l\omega_1^2}$, $d_1 = \frac{c_1}{(M+m)\omega_1}$, $d_2 = \frac{c_2}{ml^2\omega_2}$, $\mu = \frac{\nu}{\omega_1}$, $x = \frac{y}{l}$, $\dot{x} = \frac{\dot{y}}{\omega_1 l}$, $\ddot{x} = \frac{\ddot{y}}{\omega_1^2 l}$, $\gamma = \varphi$, $\dot{\gamma} = \frac{\dot{\varphi}}{\omega_2}$, $\ddot{\gamma} = \frac{\ddot{\varphi}}{\omega_2^2}$.

The dimensionless parameters of the system have the following values: $a = 0.091$, $b = 3.33$, $\alpha = 0.031$, $d_1 = 0.132$ and $d_2 = 0.02$. Both subsystems (Duffing oscillator and the pendulum) have linear resonance for $\mu = 1.0$, so around this value one can expect the appearance of the complex dynamics. Amplitude f and frequency μ of the excitation are taken as control parameters.

Chapter 3

Destabilization of pendulum

System (2.0.7) possesses three qualitatively different regimes. The first one is the regime when the oscillations of the Duffing system are not large enough to destabilize the pendulum. Hence, the pendulum is at stable steady state $\gamma = 0$. The second regime appears when pendulum destabilizes and starts oscillating. The third regime is characterized by the rotating motions of the pendulum. The transition from the stable quiescence state $\gamma = 0$ to oscillations can be understood from the theoretical point of view as the destabilization of the invariant manifold $\gamma = 0$. Indeed, the manifold $\gamma = \dot{\gamma} = 0$ is invariant with respect to (2.0.7) and the dynamics on the manifold is described by the single Duffing oscillator:

$$\ddot{x}_0 + x_0 + \alpha x_0^3 + d_1 \dot{x}_0 = f \cos \mu\tau, \tag{3.0.1}$$

with an effective mass $m + M$. The linear stability of motions on this manifold is given by the variational equation:

$$\delta\ddot{\gamma} + d_2 \delta\dot{\gamma} + \left(1 - \frac{1}{b}\ddot{x}_0(\tau)\right) \delta\gamma = 0, \tag{3.0.2}$$

which has form of a linear system with respect to the variation $\delta\gamma$, perturbed periodically by the Duffing $x_0(\tau)$. Such a parametrically perturbed system is known to possess destabilization regions (parametric resonance) when the frequency of the perturbation $x_0(\tau)$ is rationally related to the frequency of the perturbation. Since in resonances zones the Duffing oscillator is usually locked $1:1$ with the external frequency, the oscillation regions in the parameter space close to $\mu \approx 2$ (the most prominent resonance) as well as $\mu \approx 1/2$, 1, 2/3, etc. are expected.

As a result of the destabilization of pendulum, PO appear, where $x_0(\tau)$ is locked $1:1$ to the external force and $\gamma(\tau)$ to some other ratio depending on the resonance

tongue. Since after the destabilization of the pendulum, the emerged periodic solution still coexists with the unstable solution $(\gamma = 0, x_0(\tau))$, it will be called branching bifurcation. In Section 4 a two-dimensional bifurcation diagram with respect to f and $\mu$is develpoed. Branching bifurcations are shown as solid lines on this bifurcation diagram in Figs. 4.0.1(a,b) delineating the resonance tongues.

Chapter 4

Two parameters continuation

In this section two bifurcation diagrams calculated in two-parameter space: amplitude f versus frequency μ of excitation are presented. Attention is focused on bifurcations of the pendulum. Duffing system, due to excitation, is oscillating in the whole considered range of parameters. Such plots give an overview of system dynamics showing the most important periodic solutions, i.e., periodic solutions with significant area of existence. Our calculations have been performed using software for numerical continuation Auto07p [38]. As the starting points in our calculations, the steady state with $f = 0.0$ is used and follow it for different values of μ detecting the bifurcations leading to different periodic motions. Moreover, in a few cases calculations starts from periodic orbits calculated by the direct integration of eq. (2.0.7). For integration the fourth order Runge-Kutta method is used. The stability of periodic solutions is given by the set of Floquet multipliers [39].

4.1 Oscillatory solutions in plane (f, μ)

In Fig. 4.0.1(a) main resonances for which the pendulum is oscillating are shown. Different colours of bifurcation lines indicate the borders of different resonances tongues, i.e., areas with different locking ratio between the pendulum and the excitation frequency. Duffing oscillator after branching bifurcation is always locked $1:1$ with excitation frequency, further bifurcations can change this ratio. The natural dimensionless frequency of the pendulum and the Duffing oscillator are equal to one. The resonances with the following locking rations: $1:1$ (purple line), $1:2$ (orange line), $2:1$ (green line), $4:3$ (blue line), $2:5$ (yellow line), and $2:3$ (red line) were found. These borders of the resonance tongues are of two kinds. Continuous lines correspond to the destabilization of the pendulum at the branching bifurcation and the

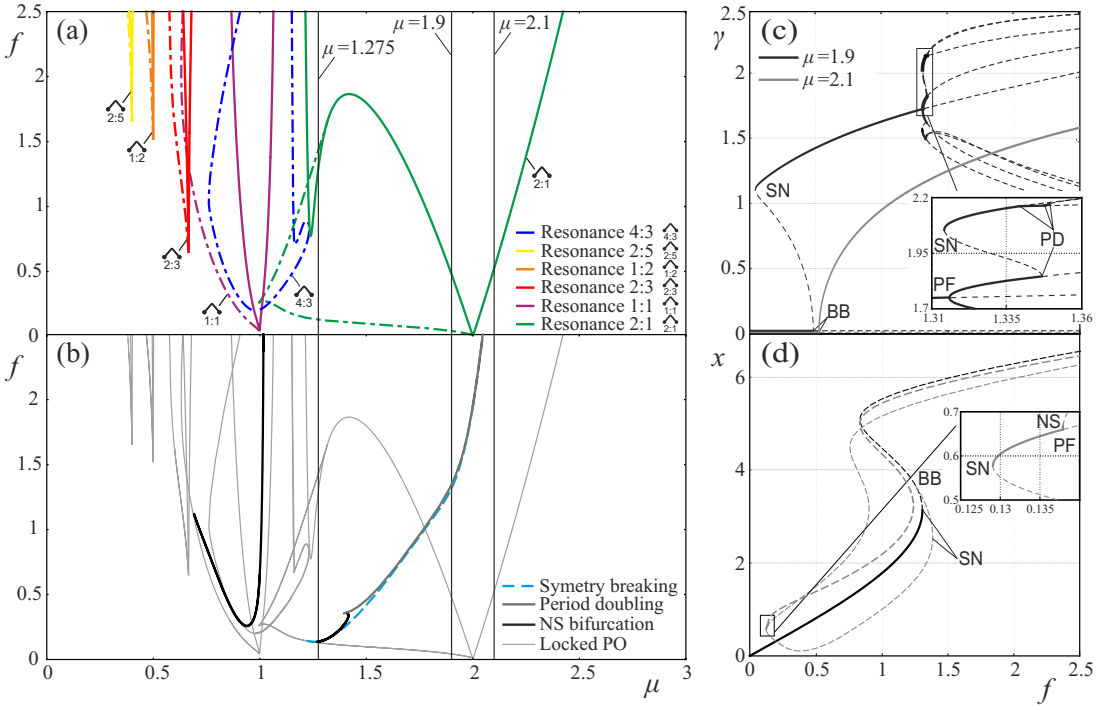

Figure 4.0.1: Bifurcation diagrams of the PO of the pendulum for system (2.0.7) in two parameter space (f, μ). (a) Tongues of resonances: solid lines correspond to the destabilization of the pendulum and birth of PO, dashed-dotted lines denote saddle-node bifurcations of PO. Different colours distinguish PO with different locking ratios between the pendulum and the excitation. (b) Bifurcation lines where the destabilization of PO occurs via symmetry breaking, period doubling, or Neimark-Saker bifurcations. (c) One-dimensional bifurcation diagrams for $\mu = 1.9$ (black lines) and $\mu = 2.1$ (grey lines) shows a route to $2:1$ resonance in more details. (d) One-dimensional bifurcation diagram ($\mu = 1.275$) for $2:1$ tongue, black line shows PO with pendulum in hanging down position and grey one with oscillating pendulum. In (c,d) solid and dashed lines correspond to stable and unstable PO respectively. Abbreviations: BB - branching bifurcation, NS - Neimark-Saker bifurcation, PF - symmetry breaking pitchfork bifurcation, SN - saddle-node bifurcation.

appearance of PO with oscillating pendulum, and dashed-dotted lines to saddle-node bifurcations of PO.

Resonance $4:3$ appears in the saddle-node bifurcation and it is stable in a large range of parameters. Other resonances have qualitatively similar structure with three bifurcation curves meeting in one point: two solid lines and one dashed-dotted. The main resonant tongues ($1:1$ and $2:1$) come very close to the axis $f = 0$ due to small friction. Illustratation of the corresponding bifurcation scenarios is shown in Fig. 4.0.1(c) using one-dimensional bifurcation diagrams for the case of $2:1$ resonance. Fig. 4.0.1(c) shows maximum amplitude of the pendulum versus f for $f \in (0.0, 2.5)$ with fixed $\mu = 1.9$ and $\mu = 2.1$. Solid and dashed lines correspond to stable and unstable PO respectively. The black line indicates PO calculated for $\mu = 1.9$. As it is easy to see, till $f = 0.479$ the pendulum is in hanging down position and only the Duffing system is oscillating. Then through the subcritical branching bifurcation PO (which corresponds to the oscillations of the pendulum) appears, but this branch of the PO is unstable (continuous line on the left side of the edge of the tongue (Fig. 4.0.1(a) indicate this bifurcation). For $f = 0.043$ the saddle-node bifurcation of PO takes place and this branch of PO stabilizes. For $f = 1.316$ one can observe the symmetry breaking pitchfork bifurcation generating two asymmetric solutions. Both branches of PO originated from pitchfork bifurcation, destabilize in the subcritical period doubling bifurcations in which the new unstable PO with doubled period is born. This branch of PO stabilizes in the saddle-node bifurcation. Especially interesting is the situation shown in the enlargement in Fig. 4.0.1(c). One can see the coexistence of the $4:1$ asymmetric PO (both Duffing and pendulum are quadruple) first with symmetric $2:1$ PO and then after symmetry breaking pitchfork bifurcation of $2:1$ resonance with two asymmetric $2:1$ PO (after this bifurcation Duffing oscillator is locked $2:1$ with excitation - the same ratio as pendulum). Further increase of f for $4:1$ asymmetric PO leads through the period doubling scenario to chaos. This bifurcation route shows that scenario described by Miles [3, 40] in the considered case of system (2.0.7) becomes more complicated.

In the same plot scenario for $\mu = 2.1$ is presened (grey line) where the lower equilibrium position of the pendulum is destabilized by the supercritical branching bifurcation for $f = 0.524$ (bifurcation takes place at continuous line on the right side of the edge of the tongue (see Fig. 4.0.1(a))) and the stability of this solution does not change in the considered range of the amplitude of excitation f.

The same scenarios, with division into right (only continuous line) and left (continuous and dashed-dotted lines) sides of the edge of the tongues are observed for other resonances (see Fig. 4.0.1(a)). In case of $2:1$ resonance branching bifurcation is a period doubling bifurcation while for other resonances branching bifurcation

leads to different locking ratios.

For 2 : 1 resonance in the range $\mu \in (1.23, 1.317)$ the continuous green line is below the dashed-dotted green line. In this area one can observe the bifurcation scenario which is shown in Fig. 4.0.1(d) for $\mu = 1.275$ in the range $f \in (0.0, 2.5)$ versus maximum amplitude of Duffing oscillator. The black solid line shows the growth of the amplitude of the Duffing oscillations in the case when the pendulum is in the lower equilibrium position. This PO loses its stability in the saddle-node bifurcation (the pendulum persists in the equilibrium position). Then the branching bifurcation of the unstable PO can be observed and the appearance of new branch of the PO for which the pendulum is in 2 : 1 resonance with excitation (grey line). After two saddle-node bifurcations the branch of the PO stabilizes for $\mu = 0.129$ (see zoom in Fig. 4.0.1d). Finally, for $\mu = 0.1378$ the PO loses its symmetry in the pitchfork bifurcation and through the Neimark-Saker bifurcation ($\mu = 0.1379$) becomes unstable.

Fig. 4.0.1(b) shows main destabilization scenarios for locked PO. The resonances tongues are marked by grey lines in the background of the plot. The Neimark-Saker bifurcations (long curve in Fig. 4.0.1(b)) destroys the 1 : 1 resonant PO, i.e., above the line of this bifurcation locked 1 : 1 PO does not exist. Other lines are connected to stability of 2 : 1 tongue. The dashed light blue line indicates the symmetry breaking pitchfork bifurcation and just after it one can observe the period doubling bifurcation (detailed route to chaos is shown in zoom in Fig. 4.0.1(c)). At the end of period doubling line the Neimark-Saker bifurcation was detected, which merges with the symmetry breaking pitchfork bifurcation and 2 : 1 resonance curve. Other PO presented in Fig. 4.0.1(a) are stable in the whole covering range but they are accessible only for carefully chosen initial conditions.

4.2 Rotation in plane (f, μ)

Fig. 4.1.1(a) shows the bifurcation diagram of rotations in two-parameter (f, μ) plane. To observe rotational solutions pendulum has to undergo a global heteroclinic bifurcation. It means that this class of solutions could not be approached by following a steady state or PO. For continuation, one has to start from an integrated PR orbit. Two kinds of PR can occur in a considered system similarly to parametrically forced pendulum. One with a constant rotational motion in one direction are called a pure rotations [8] and the second one with change of rotation direction are termed oscillations-rotations [41]. All lines presented in Fig. 4.1.1(a) are saddle-node bifurcations of PR [8, 13]. One can observe the following resonant continuous PR: three ranges of the 1 : 1 locked PR in clockwise and counter-clockwise directions

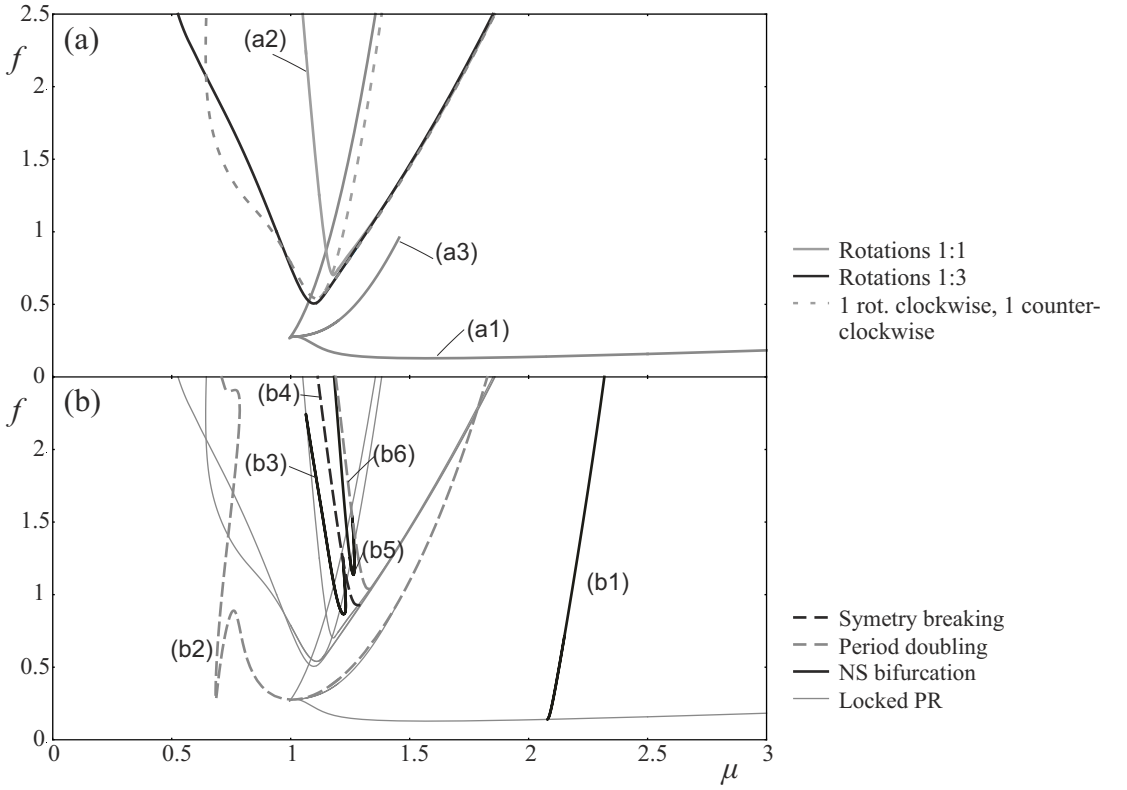

Figure 4.1.1: Bifurcation diagram of PR for system (2.0.7) in two parameter space (f,μ). Lines show bifurcations to PR with different locking ratios (a) and their destruction (b).

(solid grey), the $1:3$ in clockwise and counter-clockwise directions (solid black line). Bifurcation curves of both clockwise and counter-clockwise directions overlap due to the symmetry $\gamma \to -\gamma$. The third state is a repeated sequence of oscillations-rotations: one rotation in clockwise and one in counter-clockwise direction ($1L1R$). Fig. 4.1.1(b) shows the bifurcations which destroy PR. The $1:1$ rotational motion (solid grey line (a1)) is stable in the large range of parameters, its stability is bounded by the Neimark-Saker bifurcation (see black line (b1)) in the right part of Fig. 4.1.1(b)). The second $1:1$ area is bounded by the solid grey line (a2), with increasing parameters the Neimark-Saker bifurcation can be observed, which destabilizes this resonance (curve (b5)). The last $1:1$ PR (line (a3)) is bounded by the period doubling bifurcation curve (curve (b2)). The $1L1R$ PR goes through

the symmetry breaking pitchfork bifurcation (curve (b4)) and the period doubling bifurcation (curve (b6)) finally reaches the chaotic attractor in the period doubling cascades (the detailed description in Fig. 4.3.1(d)). The stability of $1:3$ PR is bounded, on right side, by the Neimark-Saker bifurcation (curve (b3)), where one can observe emergence of quasiperiodic motion and further transition to chaotic attractor via torus breakdown with the increase of the amplitude f. On the left side this resonance disappears in period doubling bifurcation (line (b2)).

4.3 One parameter continuation

In this section, one-parameter continuations of periodic solutions (PO as well as PR) versus the amplitude f or frequency μ of excitation is presented. Periodic solutions emerging in bifurcations presented in the previous sections are followed. In Fig. 4.3.1(a-c) maximum velocity $\dot{\gamma}$ is presented while in Fig. 4.3.1(d) maximum angular position γ. PO and PR presented in Fig. 4.3.1(a) are calculated for the frequency of excitation fixed to $\mu = 0.92$ and f is varied. When $f \in (0.0, 0.812)$ one can observe the oscillation of the Duffing oscillator while the pendulum is in the lower equilibrium position (line (1)). At the end of this interval this state loses its stability in the subcritical branching bifurcation and unstable PO is created. For $f = 0.162$ the pendulum oscillations stabilize via saddle-node bifurcation and further destabilize at $f = 0.274$ through the Neimark-Saker bifurcation (curve (2)). For this value of the frequency μ there appear rotational solutions. Line (3) corresponds to rotational resonance $1:3$ and the line (4) indicates $1L1R$ PR, both solutions appear through the saddle-node bifurcations for $f = 1.11$ and for $f = 1.0$ respectively. Line (5) shows $9:9$ resonance stable in range $f \in (0.49, 0.51)$ (this locked solution have small area of existence and it is not shown in two-dimensional bifurcations diagram).

In Fig. 4.3.1(b) the frequency is fixed as $\mu = 1.2$. One can observe a stable steady state of the pendulum in the whole range of f (line (1)). In this case, the dynamics is reduced to the motion of the forced Duffing oscillator. The $4:3$ locked oscillation for $f \in (0.628, 0.847)$ can be also observed(line (2)), which corresponds to the loop in two dimensional plot (see right side of $4:3$ resonance in Fig. 4.1.1(a)). Stable $1:1$ rotations (line (5)) in both directions appear in the first range in Neimark-Saker and become unstable in period doubling bifurcation ($f \in (0.39, 0.40)$). In the second range $1:1$ PR is stabilized by the saddle-node bifurcation and becomes unstable through the Neimark-Saker bifurcation for $f \in (0.743, 0.938)$. Last two curves are PR: $1:3$ rotation is stable from $f = 0.733$ (line (3)), and $1L1R$ motion is stable in range $f \in (0.736, 1.44)$ (line (4)).This last $1L1R$ PR disappears in symmetry

breaking pitchfork bifurcation; the detailed analysis of this PR and its bifurcations is presented in Fig. 4.3.1(d).

Fig. 4.3.1(c) shows the periodic solutions for $\mu = 2.25$. One can observe $2:1$ resonant PO (line (2)), which emerges at the branching bifurcation ($f = 1.39$) from stable steady state of the pendulum (line (1)) and stable $1:1$ rotation (line (3)) which starts at the saddle-node bifurcation and terminates in the Neimark-Saker bifurcations at the ends of the interval $f \in (0.147, 1.75)$.

The last plot (Fig. 4.3.1(d)) shows a route to chaos starting from $1L1R$ rotations for fixed value $f = 1.25$ and variable μ. For frequency $\mu = 0.80$, one can observe the saddle-node bifurcation (on line (1)), when $\mu = 1.218$ the PR goes through the symmetry breaking pitchfork bifurcation and two asymmetric $1L1R$ rotation appears (line (2)). Further the range of existence of stable two dimensional quasiperiodic solution (confirmed by integration) can be observed, which starts and ends in the Neimark-Saker ($f = 1.249$) and the inverse Neimark-Saker ($f = 1.268$) bifurcations (on line (2)). Finally, the period doubling route to chaos can be observed. Only the first solution branch with doubled period (line (3)) is shown.

4.4 Influence of non–linearity of spring

The characteristic of spring have a significant influence on transfer of energy from Duffing oscillator to the pendulum during resonances [30, 32]. Fig. 4.4.1 presents these properties for two pairs of parameters: first for $\mu = 1.0$ and $f = 0.49$ in $1:1$ resonance tongue (a) and second for $\mu = 2.0$ and $f = 1.02$ in $2:1$ resonance tongue (b). Black and grey colours indicate respectively the maximum position of mass M – x and the maximum angle of the pendulum – γ as functions of the spring non-linearity α. The continuous and dashed lines indicate respectively stable and unstable PO. It is easy to see that for $1:1$ resonance in the case of $\alpha = 0$ linear resonance occurs (Duffing oscillator is reduced to linear oscillator). For smaller values of α the amplitude of oscillations is rapidly decreasing for both pendulum and Duffing oscillator up to $\alpha = -0.97$ where the motion of the pendulum stops. Similar decrease of the amplitude of oscillations appears for positive α,but motion terminates at $\alpha = 4.05$. For $\mu = 0.05$ one can observe the Neimark-Saker bifurcation followed by the inverse Neimark-Saker bifurcation for $\mu = 0.075$. Between the bifurcation a stable quasiperiodic motion is observed. In Fig. 4.4.1(b) one observes a stable $2:1$ PO in the whole range of α. When the system is changing from soft to hard characteristic of spring amplitudes of the Duffing oscillator and the pendulum are increasing. One can not observe a resonance of Duffing system. In $1:1$ resonance a decrease of the amplitude of the oscillation of mass M can be observed, while in

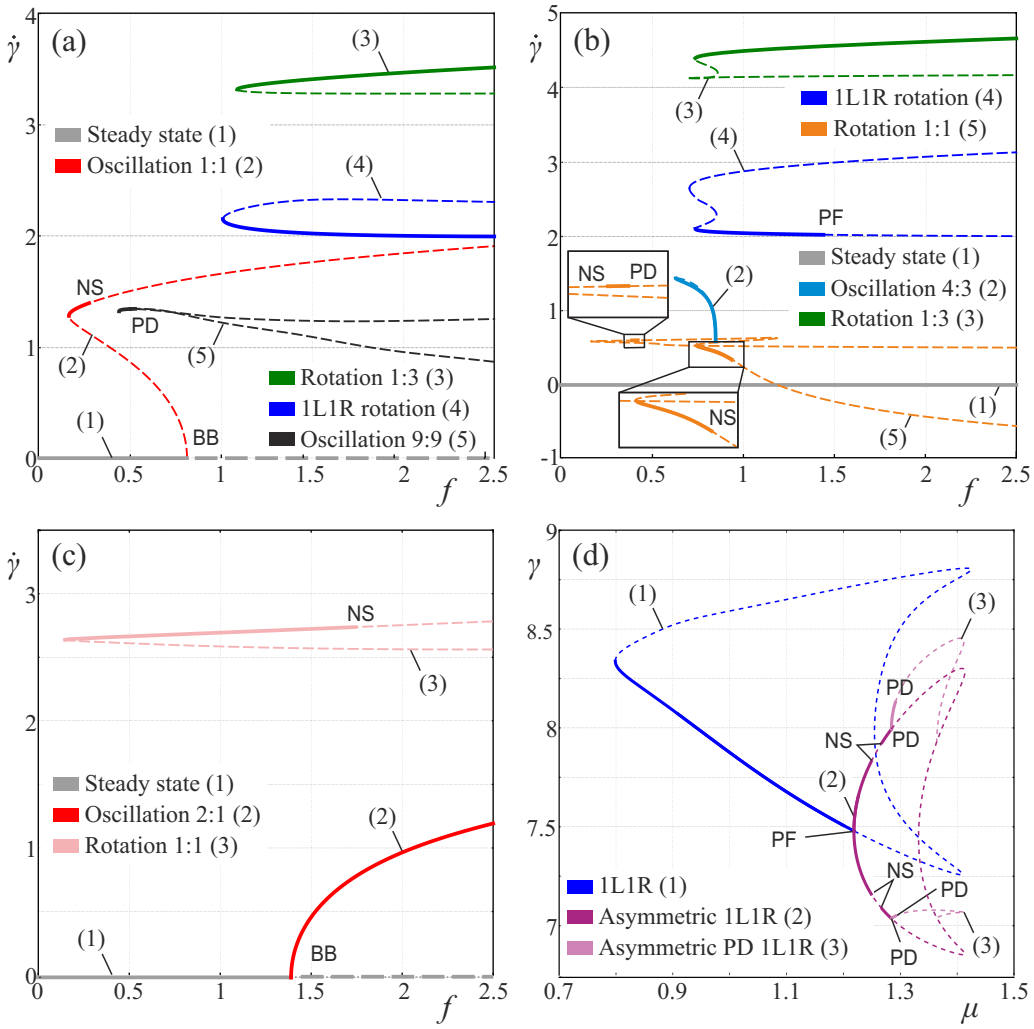

Figure 4.3.1: Continuations of periodic solutions in one parameter f for $\mu = 0.92$ (a), $\mu = 1.2$ (b), and$\mu = 2.25$ (c). (d) shows period doubling route to chaos starting from $1L1R$ rotational solution for fixed $f = 1.25$ and variable μ. Solid and dashed lines indicate the stable and unstable periodic solution respectively. Abbreviations: BB - branching bifurcation, PD - period doubling bifurcation, NS - Neimark-Saker bifurcation, PF - symmetry breaking pitchfork bifurcation. Other changes of the stability take place through the saddle-node bifurcations.

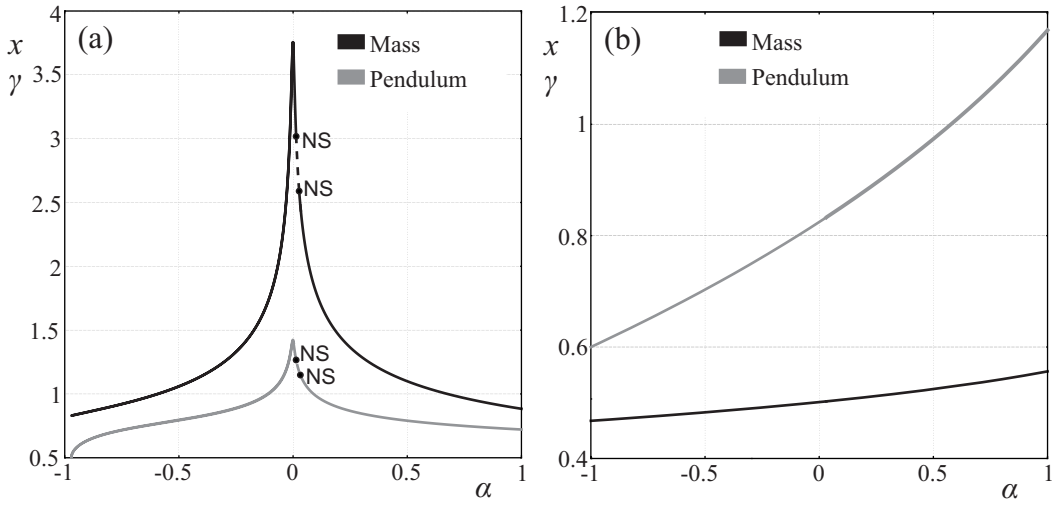

Figure 4.4.1: Maximum amplitude of mass (black) and maximum angle of pendulum (gray) versus non-linearity of spring α in range $\alpha \in (-1.0, 1.0)$ for 1:1 resonance (a) and 2:1 resonance (b). Characteristic of spring is changing from "soft" to "hard" with the increasing of α. Continuous and dashed lines indicate stable and unstable periodic solutions. Abbreviation NS indicate Neimark-Saker bifurcation.

others resonances (similarly as for $2:1$ PO) this amplitude increases due to energy transmitted from the oscillating pendulum.

Chapter 5

Coexistence of solutions

Following previous sections, see e.g. Fig. 4.3.1(a-d), multiple stable periodic solutions often coexist for the same parameter values. This section illustrates basins of attraction of different stable periodic solution. Numerical package Dynamics 2 [42] is used. Six representative sets of parameters (f, μ) were chosen and the calculated basins in plane $(\gamma, \dot{\gamma})$ are shown (angular displacement and velocity of pendulum), where γ is $\bmod 2\pi$. Initial conditions of the pendulum are taken in ranges: $\gamma \in (-\pi, \pi)$ and $\dot{\gamma} \in (4, -4)$, initial conditions of Duffing oscillator are fixed for each plot and have the following values: $x_0 = 0$, $\dot{x}_0 = 0$ (a,b,d,e), $x_0 = 2.0$, $\dot{x}_0 = 5.0$ (c, f). Since different initial conditions of the Duffing oscillator may lead to different attractors in plane $(\gamma, \dot{\gamma})$, the obtained figures show two-dimensional cross-sections of the four directional phase space (plus the phase of the perturbation). There is no guarantee that for other initial states of Duffing one can reach the same set of attractors. As one can see in Fig. 4.1.1 and Fig. 5.0.2 most of the periodic solutions are accumulated in range $\mu \in (0.7, 1.3)$, so four out of six the basins in this area were calculated. In Fig. 5.0.1(a) ($\mu = 0.9$ and $f = 0.5$) five attractors can be found: steady state, pair of period nine motion and chaotic motion which bifurcates from $1:1$ PO. Then in Fig. 5.0.1(b) ($\mu = 1.03$ and $f = 1.25$) one can observe five attractors. Two of them are symmetric pairs of rotations ($1:3$ resonance), two corresponds to symmetric $1:1$ PO and the last one is the $1L1R$ PR. Next plot ($\mu = 1.2$ and $f = 0.75$) includes seven attractors: two symmetric pairs of PR ($1:1$ and $1:3$), $4:3$ PO, equilibrium of pendulum and $1L1R$ PR. In Fig. 5.0.1(d) ($\mu = 1.229$ and $f = 1.0$) six solutions were detected, two of them are quasiperiodic bifurcated from symmetric pair of $1:1$ PR , pair of $1:3$ PR, steady state of pendulum and $1L1R$ PR. For larger values of excitation one can also find chaotic attractor, e.g. for $\mu = 1.6$, $f = 1.95$ (see Fig. 5.0.1(e)). Usually the chaotic solution dominates the whole phase space and

the coexisting attractors have small basins of attraction and such a situation is also observed in the investigated system (2.0.7).The last Fig. 5.0.1(f) shows a case where one do not observe fractal basins of attraction. Most of the phase space is dominated by period two symmetric PO, only in small range one can see basins of symmetric pair of $1:1$ PR.

Generally, in area where $1L1R$ PR exists its basin of attraction dominates in phase space. The $4:3$ resonance could be observed for all pairs of parameters used in Fig. 5.0.1(a-d). Nevertheless, one can see this attractor only in Fig. 5.0.1(c) where different initial conditions of Duffing are used. This is the evidence that not only sensitivity on initial state is observed for pendulum but also for Duffing. Varying initial condition of Duffing moves cross-section of the phase space and changes the set of accessible attractors.

Almost all basins of attraction have a fractal structure so reaching the given solution is strongly dependent on initial conditions. From the practical point of view it is important to know the area with a small number or even one solution [43]. In such ranges one can be sure that the system approaches the expected solution. In Fig. 5.0.2 the areas with different types of attractors are marked: black colour indicates one attractor (four locked PO, excluding $4:3$ resonance, between two branching bifurcation lines on the left and right side - the edges of the resonance tongues), grey colour refers to two coexisting solutions (the same as for black but with coexisting steady state of the pendulum). In the hatched area one observe the coexistence of PR (two symmetric pairs of $1:1$ or $1:3$ or $1L1R$ PR) and the steady state of the pendulum. The largest area with one attractor is a tongue of $2:1$ resonance. For other resonances ($1:1$, $2:3$, $2:5$, $1:2$) these areas are small. Especially, it is surprising for $1:1$ where the resonance tongue is large in the parameter space but only near its edge one do not find the second attractor. Areas where only Duffing system is oscillating and pendulum is in stable equilibrium position are not marked. In this case the dynamics of the system is reduced to the oscillations of mass $(M+m)$.

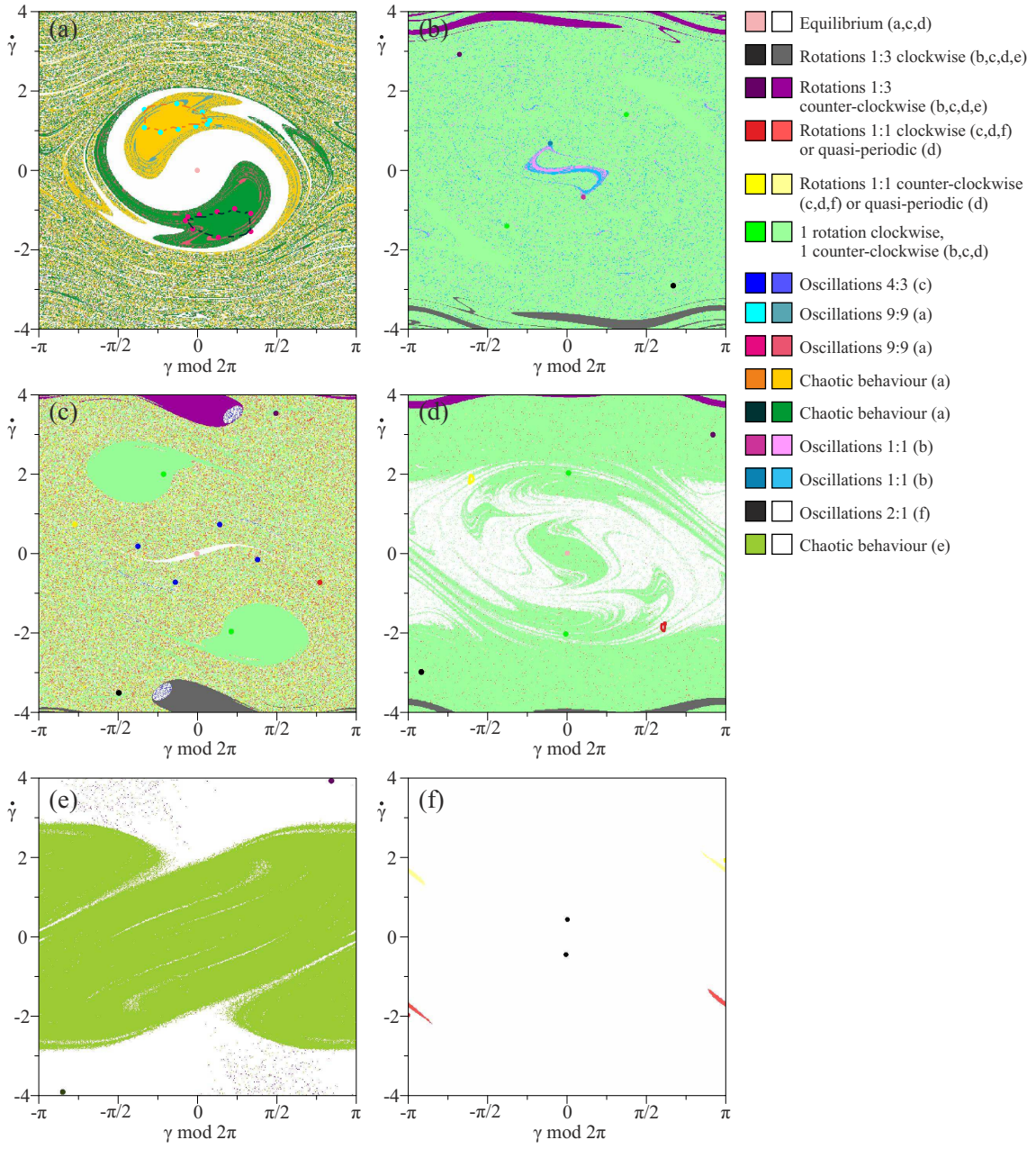

Figure 5.0.1: Basins of attraction in the plane of the pendulum variables $(\gamma, \dot{\gamma})$ for $\mu = 0.9$, $f = 0.5$ (a); $\mu = 1.03$, $f = 1.25$ (b); $\mu = 1.2$, $f = 0.75$ (c); $\mu = 1.229$, $f = 1.0$ (d); $\mu = 1.6$, $f = 1.95$ (e), and $\mu = 2.37$, $f = 2.25$ (f). The colours for attractors their basins are shown in legend.

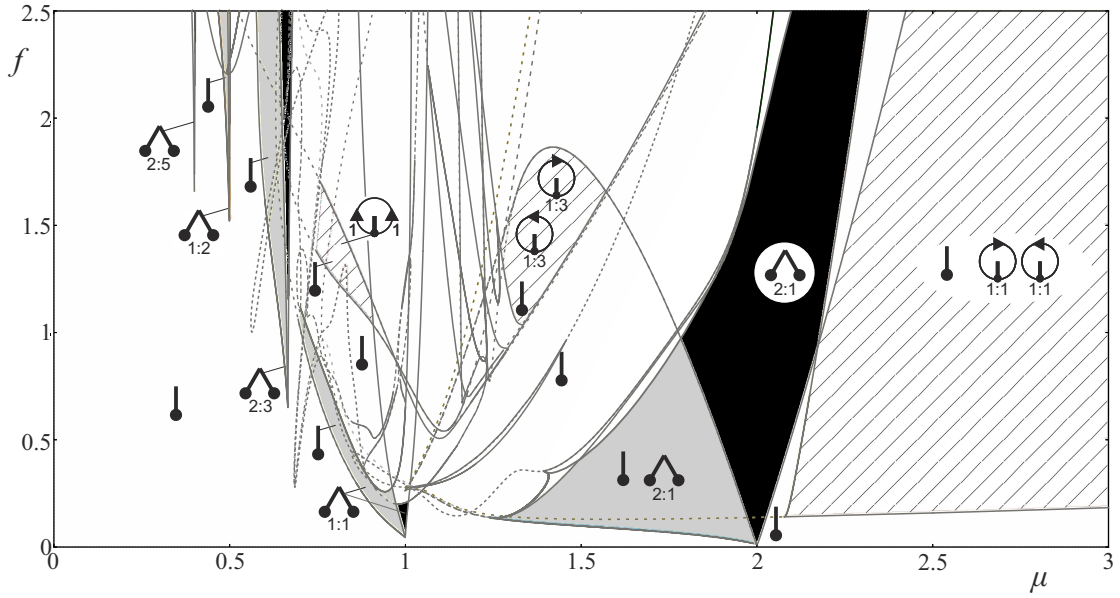

Figure 5.0.2: Two-parameter bifurcations diagram in plane (f, μ) with PO and PR. Black colour indicates one attractor (for locked PO, excluding $4:3$ resonance, between period doubling bifurcation lines on the left and right side - edges of the resonance tongues), gray colour shows two coexisting attractors (the same as for black but with coexisting stable steady state of the pendulum). In the hatched area one can observe the coexistence of stable rotations (three areas with: pairs of symmetric $1:1$ or $1:3$ or $1L1R$ PR) and stable steady state of the pendulum.

Chapter 6

Conclusions

Comprehensive numerical analysis of the forced Duffing oscillator with the suspended pendulum is presented in this thesis. Two dimensional bifurcation diagrams with the most representative periodic solutions and demonstrate the bifurcation route to the locked resonances are shown. The linear resonance of both subsystems is observed for $\mu = 1.0$ and around this value complex dynamics with many coexisting attractors was found, not only periodic but also quasiperiodic and chaotic ones. In the principal resonance zone the pendulum oscillations decrease the oscillation amplitude of the Duffing oscillator so one can observe an energy transfer from the Duffing oscillator to the pendulum. These properties are observed only for $1:1$ oscillatory resonance, for other locked solutions (oscillations or rotations) the pendulum oscillations increase the oscillations amplitude of the Duffing oscillator (the control and the possible decrease of the amplitude for other resonances will be considered in future work). Contrary to complex dynamics around $1:1$ principal resonance in the neighbourhood of $2:1$ parametric resonance, two large ranges in parameters space with only one attractor were found ($2:1$ locked oscillations) and symmetric pair of $1:1$ rotations respectively. From the practical point of view (certainty of reaching the desired attractor) such a situation is very useful and rare in non–linear system.

The influence of non-linearity of spring on the amplitude of oscillations For principal $1:1$ resonance was also compared, strong non-linearity (hardening or softening) causes lower amplitude of oscillations. For $2:1$ parametric resonance only the decrease of α into the softening direction causes the decrease of the oscillations amplitude. The existence of fractal basins of attraction is not surprising for non–linear systems with the attached pendulum. Hence, one can consider only the probability of reaching the chosen attractor and never have a certainty where the dynamics of systems evolves. This is crucial when the pendulum is working as a tune mass

absorber so the areas with a low number of coexisting solutions in the parameters space are shown.

Bibliography

[1] R.W. Leven, B.P. Koch, Chaotic behaviour of a parametrically excited damped pendulum, Physics Letters A 86 (2) (1981) 71 – 74.

[2] R.W. Leven, B. Pompe, C. Wilke, B.P. Koch, Experiments on periodic and chaotic motions of a parametrically forced pendulum, Physica D Nonlinear Phenomena 16 (1985) 371–384.

[3] J. Miles, Resonance and symmetry breaking for the pendulum, Phys. D 31 (1988) 252–268.

[4] P.J. Bryant, J.W. Miles, On a periodically forced, weakly damped pendulum. part 3: vertical forcing., Journal of the Australian Mathematical Society, Series B 32 (1990) 42–60.

[5] P.J. Bryant, J.W. Miles, On a periodically forced, weakly damped pendulum. part 1: applied torque., Journal of the Australian Mathematical Society, Series B 32 (1990) 1–22.

[6] P.J. Bryant, J.W. Miles, On a periodicaly forced, weakly damped pendulum. part 2: Horizontal forcing, Journal of the Australian Mathematical Society, Series B 32 (1990) 23–41.

[7] S.R. Bishop, M.J. Clifford, The use of manifold tangencies to predict orbits, bifurcations and estimate escape in driven systems, Chaos, Solitons and Fractals 7 (10 SPEC. ISS.) (1996) 1537–1553.

[8] M. Clifford, S. Bishop, Rotating periodic orbits of the parametrically excited pendulum, Physics Letters A 201 (2-3) (1995) 191–196, cited By (since 1996) 17.

[9] B. Horton, J. Sieber, J. Thompson, M. Wiercigroch, Dynamics of the nearly parametric pendulum, International Journal of Non-Linear Mechanics 46 (2) (2011) 436 – 442.

[10] X. Xu, M. Wiercigroch, Approximate analytical solutions for oscillatory and rotational motion of a parametric pendulum, Nonlinear Dynamics 47 (1-3) (2007) 311–320.

[11] J.-W Liang Identifying Coulomb and viscous damping from free-vibration acceleration decrements. J. Sound Vib. 282 (2005) 1208–1220.

[12] J.-W Liang, B.F Feeny Balancing energy to estimate damping parameters in forced oscillators. J. Sound Vib. 295 (2006) 988–998.

[13] X. Xu, M. Wiercigroch, M.P. Cartmell, Rotating orbits of a parametrically-excited pendulum, Chaos, Solitons and Fractals 23 (5) (2005) 1537–1548.

[14] B. Banerjee, A.K. Bajaj, P. Davies , Resonant dynamics of an autoparametric system: A study using higher-order averaging, International Journal of Non-Linear Mechanics 31 (1) (1996) 21–39.

[15] O. Kholostova, Some problems of the motion of a pendulum when there are horizontal vibrations of the point of suspension, Journal of Applied Mathematics and Mechanics 59 (4) (1995) 553–561.

[16] S.-Y. Kim, S.-H. Shin, J. Yi, C.-W. Jang, Bifurcations in a parametrically forced magnetic pendulum, Physical Review E - Statistical Physics, Plasmas, Fluids, and Related Interdisciplinary Topics 56 (6) (1997) 6613–6619.

[17] S. Kim, K. Lee, Multiple transitions to chaos in a damped parametrically forced pendulum, Physical Review E 53 (1995) 1579–1586.

[18] J. Liu. R. Kobes, S. Peles, Analysis of a parametrically driven pendulum, Physical Review E 63 (2000) 036219–17.

[19] J.L. Trueba, J.P. Baltanas, M.A.F Sanjuan,, A generalized perturbed pendulum, Chaos, Solitons and Fractals 15 (5) (2003) 911–924.

[20] A. Sofroniou, S.R. Bishop, Breaking the symmetry of the parametrically excited pendulum, Chaos, Solitons and Fractals 28 (3) (2006) 673–681.

[21] B. Horton, X. Xu, M. Wiercigroch, Transient tumbling chaos and damping identification for parametric pendulum, Philosophical Transactions of the Royal Society of London, A 366 (2007) 767–784.

[22] X. Xu, E. Pavlovskaia, M. Wiercigroch, F. Romeo, S. Lenci, Dynamic interactions between parametric pendulum and electro-dynamical shaker, ZAMM Zeitschrift fur Angewandte Mathematik und Mechanik 87 (2) (2007) 172–186.

[23] F. Verhulst, A. Tondl, T. Ruijgork, R. Nabergoj, Autoparametric Resonance in Mechanical System, Cambridge University Press, New York, 2000.

[24] A. Gus'kov, G. Panovko, C. Van Bin, Analysis of the dynamics of a pendulum vibration absorber, Journal of Machinery Manufacture and Reliability 37 (2008) 321–329.

[25] H. Hatwal, A. K. Mallik, A. Ghosh, Forced nonlinear oscillations of an autoparametric system—part 1: Periodic responses, Journal of Applied Mechanics 50 (3) (1983) 657–662.

[26] H. Hatwal, A. K. Mallik, A. Ghosh, Forced nonlinear oscillations of an autoparametric system—part 2: Chaotic responses, Journal of Applied Mechanics 50 (3) (1983) 663–668.

[27] A.K. Bajaj, S.I. Chang, J.M. Johnson, Amplitude modulated dynamics of a resonantly excited autoparametric two degree-of-freedom system, Nonlinear Dynamics 5 (1994) 433–457.

[28] J.M. Balthazar, B.I. Cheshankov, D.T. Ruschev, L. Barbanti, H.I. Weber, Remarks on the passage through resonance of a vibrating system with two degrees of freedom, excited by a non-ideal energy source, Journal of Sound and Vibration 239 (5) (2001) 1075–1085.

[29] M.P. Cartmell, J. Lawson, Performance enhancement of an autoparametric vibration absorber by means of computer control, Journal of Sound and Vibration 177 (2) (1994) 173–195.

[30] K. Kecik J. Warminski, Autoparametric vibration of a nonlinear system with pendulum, Mathematical Problems in Engineering 2006 (2006) 80705.

[31] Y. Song, H. Sato, Y. Iwata, T. Komatsuzaki, The response of a dynamic vibration absorber system with a parametrically excited pendulum, Journal of Sound and Vibration 259 (4) (2003) 747–759.

[32] J. Warminski, K. Kecik, Instabilities in the main parametric resonance area of a mechanical system with a pendulum, Journal of Sound and Vibration 322 (3) (2009) 612 – 628, Special issue from the Second International Conference on

Nonlinear Dynamics, Kharkov, Ukraine, 25-28 September 2007, held in honour of the 150th anniversary of Alexander M. Lyapunov, Second International Conference on Nonlinear Dynamics.

[33] J. Warminski, J. Balthazar, R. Brasil, Vibrations of a non-ideal parametrically and self-excited model, Journal of Sound and Vibration 245 (2) (2001) 363 – 374.

[34] K. Kecik, J. Warminski, Dynamics of an autoparametric pendulum-like system with a nonlinear semiactive suspension, Mathematical Problems in Engineering.

[35] B. Vazquez-Gonzalez, G. Silva-Navarro, Evaluation of the autoparametric pendulum vibration absorber for a duffing system, Shock and Vibration 15 (2008) 355–368.

[36] L. Macias-Cundapi, G. Silva-Navarro, B. Vazquez-Gonzalez, Application of an active pendulum-type vibration absorber for duffing systems, in: Electrical Engineering, Computing Science and Automatic Control, 2008. CCE 2008. 5th International Conference on, 2008, pp. 392 –397.

[37] T. Ikeda, Nonlinear responses of dual-pendulum dynamic absorbers, Journal of Computational and Nonlinear Dynamics 6 (1) (2011) 011012.

[38] E.J. Doedel, A.R. Champneys, T.F. Fairgrieve. Y.A. Kuznetsov, B. Sandstede, X. Wang Auto 97: continuation and bifurcation software for ordinary differential equations (1998).

[39] Y. Kuznetsov, Elements of Applied Bifurcation Theory, Vol. 112 of Applied Mathematical Sciences, Springer-Verlag, 1995.

[40] J. Miles, Resonance and symmetry breaking for as duffing oscillator, SIAM J. Appl. Math. 49 (1989) 968–981.

[41] W. Szemplinska-Stupnicka, E. Tyrkie, The oscillation-rotation attractors in the forced pendulum and their peculiar properties, Int. J. Bifurcation and Chaos 12 (2002) 159–68.

[42] J. Yorke, H.E. Nusse, Dynamics: numerical explorations, second, revised and enlarged edition Edition, Vol. 101 of Applied Mathematical Sciences, Springer-Verlag, New York, Inc., 1998.

[43] A. Chudzik, P. Perlikowski, A. Stefanski, T. Kapitaniak, Multistability and rare attractors in van der pol-duffing oscillator., I. J. Bifurcation and Chaos 21 (7) (2011) 1907–1912.